



HAL
open science

The Fat Boundary Method: Semi-Discrete Scheme and Some Numerical Experiments

Silvia Bertoluzza, Mourad Ismail, Bertrand Maury

► **To cite this version:**

Silvia Bertoluzza, Mourad Ismail, Bertrand Maury. The Fat Boundary Method: Semi-Discrete Scheme and Some Numerical Experiments. DOMAIN DECOMPOSITION METHODS IN SCIENCE AND ENGINEERING, springer, pp.513, 2005, Lecture Notes in Computational Science and Engineering. hal-00666064

HAL Id: hal-00666064

<https://hal.science/hal-00666064>

Submitted on 3 Feb 2012

HAL is a multi-disciplinary open access archive for the deposit and dissemination of scientific research documents, whether they are published or not. The documents may come from teaching and research institutions in France or abroad, or from public or private research centers.

L'archive ouverte pluridisciplinaire **HAL**, est destinée au dépôt et à la diffusion de documents scientifiques de niveau recherche, publiés ou non, émanant des établissements d'enseignement et de recherche français ou étrangers, des laboratoires publics ou privés.

The Fat Boundary Method: Semi-Discrete Scheme and Some Numerical Experiments

Silvia Bertoluzza¹, Mourad Ismail², and Bertrand Maury³

¹ Istituto di Matematica Applicata e Tecnologie Informatiche del C.N.R.
v. Ferrata 1, 27100 Pavia. Italy. (silvia.bertoluzza@imati.cnr.it).

² Laboratoire Jacques-Louis Lions, Université Pierre et Marie Curie.
Boîte courrier 187, 75252 Paris Cedex 05. France. (ismail@ann.jussieu.fr).

³ Laboratoire de Mathématiques, Université Paris-Sud.
Bâtiment 425, 91405 Orsay. France. (bertrand.maury@math.u-psud.fr).

Summary. The **Fat Boundary Method (FBM)** is a fictitious domain like method for solving partial differential equations in a domain with holes $\Omega \setminus \overline{B}$ - where B is a collection of smooth open subsets - that consists in splitting the initial problem into two parts to be coupled via Schwartz type iterations: the solution, with a fictitious domain approach, of a problem set in the whole domain Ω , for which fast solvers can be used, and the solution of a collection of independent problems defined on narrow strips around the connected components of B , that can be performed fully in parallel. In this work, we give some results on a semi-discrete **FBM** in the framework of a finite element discretization, and we present some numerical experiments.

1 The Fat Boundary Method

The Fat Boundary Method (**FBM**) was introduced by Maury [2001] to solve partial differential equations in a domain with holes. For simplicity we present the method in the case of the Poisson problem. Let us denote by $\Omega \subset \mathbb{R}^n$ a Lipschitz bounded domain and $B \subset \Omega$ a collection of smooth subsets (typically balls). The boundaries of Ω and B are respectively denoted by Γ and γ . Our purpose is to solve the problem: Find $u \in H_0^1(\Omega \setminus \overline{B})$, such that

$$-\Delta u = f \text{ in } \Omega \setminus \overline{B}. \quad (1)$$

Solving this problem by **FBM** consists in splitting it into a local resolution in a neighborhood of B , where we can use a fine mesh (in a thin layer around the holes, the dashed subdomain denoted by ω in figure 1), and a global resolution based on a cartesian mesh covering the whole domain Ω . This makes it possible the use of fast solvers and good preconditioners.

The link between the global and the local problem is based on the interpolation of a globally defined field on an artificial boundary which delimits the

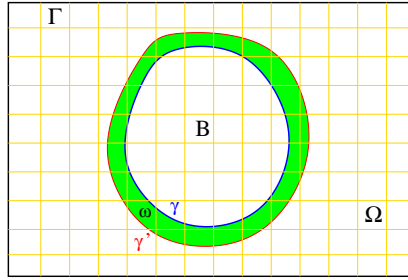


Fig. 1. Domains in the two-dimensional case

local subdomain, and the prescription of the jump of the normal derivative across the boundary of B . More precisely, we introduce a smooth artificial boundary γ' around B , and we denote by ω the (narrow) domain delimited by γ and γ' ($\partial\omega = \gamma \cup \gamma'$). We then introduce the functional space

$$H_\gamma^1(\omega) = \{v \in H^1(\omega), \quad v|_\gamma = 0\}. \tag{2}$$

We can replace problem (1) by two coupled new problems, one of which is set in ω , and the other one in the whole domain Ω : Find $(\hat{u}, v) \in H_0^1(\Omega) \times H_\gamma^1(\omega)$, such that

$$\begin{cases} a: & \begin{cases} -\Delta v = f & \text{in } \omega, \\ v = \hat{u} & \text{on } \gamma', \end{cases} \\ b: & -\Delta \hat{u} = \bar{f} + \frac{\partial v}{\partial n} \delta_\gamma & \text{in } \Omega, \end{cases} \tag{3}$$

where \bar{f} is the extension of f by 0 in B , and where $\frac{\partial v}{\partial n} \delta_\gamma \in H^{-1}(\Omega)$ stands for the continuous linear form: $w \in H_0^1(\Omega) \mapsto \int_\gamma \frac{\partial v}{\partial n} w$. More precisely, we have this result (Maury [2001])

Theorem 1. *Problems (1) and (3) are equivalent, i.e.*

- *If u is a solution of (1), then the couple $(\bar{u}, u|_\omega)$ is a solution of (3).*
- *If (\hat{u}, v) is a solution of (3), then $\hat{u}|_{\Omega \setminus \bar{B}}$ is a solution of (1).*

The local problem (3-a) and the global one (3-b) are coupled, and this suggests the use of a fixed point algorithm. Let $\theta \in]0, 1[$ be a relaxation parameter. We introduce the following operators: $\mathcal{T}_\theta(\cdot, \cdot; f): H_0^1(\Omega) \times H_\gamma^1(\omega) \longrightarrow H_0^1(\Omega) \times H_\gamma^1(\omega)$ defined by $\mathcal{T}_\theta(\hat{u}, v; f) = (\hat{U}, V)$ where $V \in H_\gamma^1(\omega)$ and $\hat{U} \in H_0^1(\Omega)$ are solutions of

$$-\Delta V = f \text{ in } \omega, \quad V = \theta v + (1 - \theta)\hat{u} \text{ on } \gamma', \tag{4}$$

$$-\Delta \hat{U} = \bar{f} + \frac{\partial V}{\partial n} \delta_\gamma \text{ in } \Omega. \tag{5}$$

By definition of \mathcal{T}_θ , (\hat{u}, v) is solution of (3) if and only if $\mathcal{T}_\theta(\hat{u}, v; f) = (\hat{u}, v)$. The following convergence result holds. (See Maury [2001] for the proof)

Theorem 2. *There exists $\theta_0 < 1$ such that for all $\theta \in]\theta_0, 1[$ the fixed point procedure*

$$(\hat{u}^{n+1}, v^{n+1}) = \mathcal{T}_\theta(\hat{u}^n, v^n; f)$$

converges to the fixed point of the operator $\mathcal{T}_\theta(\cdot, \cdot; f)$.

2 The semi-discrete case

A preliminary step towards the analysis of the discrete **FBM** – where both (4) and (5) are solved numerically – consists in assuming that the local problem (4) is solved exactly, and in focusing then on the discretization of the global problem (5). Letting $\mathbb{U}_h \subset H_0^1(\Omega)$ be a finite dimensional approximation space of finite element type, we propose the following semi-discrete fixed point iteration scheme: let $\mathcal{T}_\theta^h(\cdot, \cdot; f) : \mathbb{U}_h \times H_\gamma^1(\omega) \rightarrow \mathbb{U}_h \times H_\gamma^1(\omega)$ be defined by $\mathcal{T}_\theta^h(u_h, v; f) = (U_h, V)$ with $V \in H_\gamma^1(\omega)$ and $U_h \in \mathbb{U}_h$ respectively defined by

$$-\Delta V = f \text{ in } \omega, \quad V = \theta v + (1 - \theta)u_h \text{ on } \gamma', \tag{6}$$

$$\int_\Omega \nabla U_h \cdot \nabla w_h = \int_\Omega \bar{f} w_h + \int_\gamma \frac{\partial V}{\partial n} w_h \quad \forall w_h \in \mathbb{U}_h. \tag{7}$$

We are interested in studying the existence and uniqueness properties of the solution to the fixed point equation

$$(u_h, v^*) = \mathcal{T}_\theta^h(u_h, v^*; f), \tag{8}$$

as well as in giving an estimate on the error $u - u_h$ in Ω .

We briefly sketch here the main steps of the analysis. The first step, in order to analyze the scheme (8) is to introduce an auxiliary fixed point problem. Let us denote by $\pi_h : H_0^1(\Omega) \rightarrow \mathbb{U}_h$ the Galerkin Projection defined by

$$\int_\Omega \nabla(\pi_h u) \cdot \nabla w_h = \int_\Omega \nabla u \cdot \nabla w_h, \quad \forall w_h \in \mathbb{U}_h. \tag{9}$$

Let, for $\theta \in (0, 1)$, $\mathcal{T}_\theta^*(\cdot, \cdot; f) : H_0^1(\Omega) \times H_\gamma^1(\omega) \rightarrow H_0^1(\Omega) \times H_\gamma^1(\omega)$ be defined as follows: $\mathcal{T}_\theta^*(u, v; f) = (U, V)$ with $(U, V) \in H_0^1(\Omega) \times H_\gamma^1(\omega)$ solution to

$$-\Delta V = f \text{ in } \omega, \quad V = \theta v + (1 - \theta)\pi_h u \text{ on } \gamma', \tag{10}$$

$$-\Delta U = \bar{f} + \frac{\partial V}{\partial n} \delta_\gamma, \quad \text{in } \Omega. \tag{11}$$

Then we consider the problem

$$(u^*, v^*) = \mathcal{T}_\theta^*(u^*, v^*; f). \tag{12}$$

The relation between (12) and (8) is the object of the following lemma (Bertoluzza et al.).

Lemma 1. *Let (u^*, v^*) be a solution to the auxiliary fixed point problem (12). Then $(\pi_h u^*, v^*)$ is a solution to problem (8). Respectively let (u_h, v^*) be a solution to problem (8) then, letting $u^* \in H_0^1(\Omega)$ be the unique solution to*

$$-\Delta u^* = \bar{f} + \frac{\partial v^*}{\partial n} \delta_\gamma, \quad \text{in } \Omega, \tag{13}$$

(u^, v^*) is a solution of problem (12).*

The key ingredient of the analysis of the auxiliary problem is the following lemma (Bertoluzza et al.), stating that, under suitable assumptions the operator $\mathcal{T}_\theta^*(\cdot, \cdot; 0)$ is a contraction, and whose proof is heavily based on functions which are harmonic in $\Omega \setminus \gamma$.

Lemma 2. *Let $(u, v) \in \mathcal{R}(\mathcal{T}_\theta^*)$, and let $(U, V) = \mathcal{T}_\theta^*(u, v; 0)$. Then, if the provided h is sufficiently small, there exists $\theta_0 \in]0, 1[$ such that if $\theta > \theta_0$, for some positive $k < 1$, $|U|_{1,\Omega} \leq k|u|_{1,\Omega}$, and $|V|_{1,\omega} \leq \theta|v|_{1,\omega} + C|u|_{1,\Omega}$.*

Existence and uniqueness of the solution of the auxiliary problem (12) (and therefore, thanks to Lemma 1 of the original semidiscrete problem (8)) easily follows. Let us now estimate the error $\hat{u} - u_h$. Since the mesh is a priori chosen independently of the position of γ , it is clear that, since \hat{u} has on γ a discontinuity of the normal derivative the best global regularity that we can expect of \hat{u} is $\hat{u} \in H^{3/2-\epsilon}(\Omega)$ and therefore the best error estimate that we can expect is $\|\hat{u} - u_h\|_{1,\Omega} \leq Ch^{1/2-\epsilon}\|u\|_{3/2-\epsilon}$ (h denoting the mesh size of the triangulation which we assume to be regular and quasiuniform). However, assuming that ∂B is sufficiently regular, if $f|_{\Omega \setminus \bar{B}} \in H^{s-2}$ the function $\hat{u} = u$ is in $H^s(\Omega \setminus \bar{B})$ and then, using the technique introduced by Nitsche and Schatz [1974] in order to estimate local convergence rates, we can hope for a better convergence rate in any open set Ω^* strictly embedded in $\Omega \setminus \bar{B}$. More precisely, assuming that we are using finite elements of order m (either P_m or Q_m) the following theorem holds (Bertoluzza et al.)

Theorem 3. *Assume that $f \in H^{s-2}(\Omega \setminus \bar{B})$, with $2 \leq s \leq m + 1$, and let $\Omega^* \subset\subset \Omega$. Then, for h sufficiently small we have*

$$\|u - u_h\|_{1,\Omega^*} \leq Ch^s \|f\|_{s-2,\Omega \setminus \bar{B}}$$

3 Numerical Experiments and Conclusions

We want to verify that, as stated by Theorem 3, if we use P1 finite elements, **FBM** is of order one in every subdomain $\tilde{\Omega} \subset\subset \Omega \setminus \bar{B}$. Figure 2 shows the dependence of the errors (in H^1 and L^2 norms) upon the mesh step size h . All tests are carried out using an uniform cartesian grid. We denote global errors the ones computed in the whole domain Ω and local errors the ones computed in the subdomain $\tilde{\Omega}$ of $\Omega \setminus \bar{B}$. The domain Ω is the box $] -\frac{1}{2}, \frac{1}{2}[^3$, the ‘‘hole’’

B is the ball $B(0, R)$, where $R = 0.25$, and the subdomain $\tilde{\Omega}$ is $\Omega \setminus B(0, 0.3)$. The exact solution u is chosen to be equal to $\sin(2\pi(x^2 + y^2 + z^2 - R^2))$. The analytical solution was selected to be radial in order to eliminate the error due to the local resolution, and thus to be in conformity with the theoretical result.

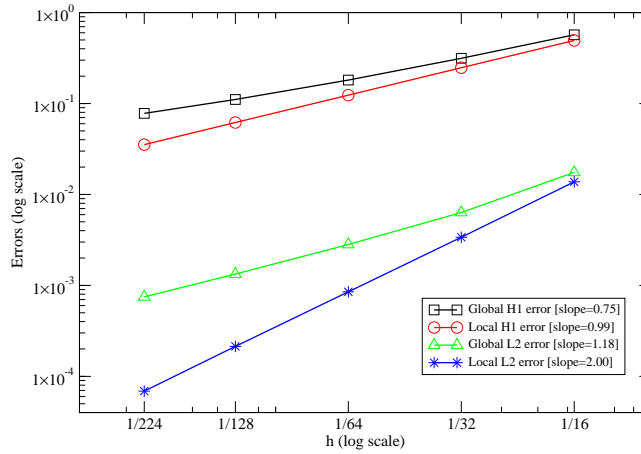


Fig. 2. Errors plots.

3.1 Capability to deal with many holes

This numerical experiment illustrates the capability to deal with a domain with “many” holes. We consider the box $] - 1, 1[^3$ with 163 disjoint balls disposed in a pseudo-random way. Figure 3-(left) shows the isosurface $u = 0$ of the computed solution, which solves the problem: $-\Delta u = 1$ in $\Omega \setminus \overline{B}$ and $u = 0$ on $\partial(\Omega \setminus \overline{B}) = \Gamma \cup \gamma$. Figure 3-(right) shows the same experiment but with a little larger number of particles: 343 balls disposed in a structured way.

3.2 Numerical Simulation of convection-diffusion around two moving balls

We consider a parallelepiped Ω in which there are two moving rigid balls $B_1 \cup B_2 = B$. Their trajectories are imposed in advance. On five faces of the box we maintain a temperature equal to 1 and at the sixth face we take homogeneous Neumann boundary conditions. On the surfaces of the two balls we impose (via Dirichlet boundary condition) a null temperature. Heat is convected using a potential field. One expects to have a “trail” of “fresh zones” following the balls in their movements. The problem we solve is the following



Fig. 3. Isosurface $u = 0$: (left)- 163 balls. (Right)- 343 balls

$$\begin{cases} \frac{\partial T}{\partial t} - \nu \Delta T + \nabla \phi \cdot \nabla T = 0 \text{ in } \Omega \setminus B, \\ T = 0 \text{ on } \gamma, \\ T = 1 \text{ on } \Gamma \setminus (z = z_{min}), \\ \frac{\partial T}{\partial n} = 0 \text{ on } (z = z_{min}), \end{cases} \quad (14)$$

where ϕ solves

$$\begin{cases} -\Delta \phi = 0 \text{ in } \Omega \setminus B, \\ \frac{\partial \phi}{\partial n} = 0 \text{ on } \gamma, \\ \frac{\partial \phi}{\partial n} = 0 \text{ on } \Gamma \setminus (z = z_{min}, z = z_{max}), \\ \phi = 1 \text{ on } (z = z_{min}), \\ \phi = 1 \text{ on } (z = z_{max}). \end{cases} \quad (15)$$

Figure 4 shows the computed solution at different time iterations.

3.3 Flow past a sphere

We consider the incompressible Navier-Stokes equations in the parallelepiped $\Omega =]-\frac{3}{2}, \frac{3}{2}[\times]-\frac{3}{2}, \frac{3}{2}[\times]-1, 5[$ containing a spherical obstacle $B((0, 0, 1), \frac{1}{2})$. The time discretisation is done using the Finite-Element Projection/Lagrange-Galerkin method (see Achdou and Guermond [2000]) which is a projection algorithm combined with the characteristics method (see Pironneau [1982]). At each time step we have to solve, by **FBM**, elliptic problems for the velocity and the pressure. Figure 5 shows the velocity field on the plan $y = 0$ of a flow past a sphere at Reynold's number equal to 100. In order to see the vortices, figure 6 presents a zoom close to the sphere. See Ismail [2003] for more details on numerical simulations of flows past spheres.

3.4 Conclusions

The numerical results confirm the theoretical estimates and shows the wide applicability of **FBM**. The future work will consist on the theoretical side in taking into account also the error due to the local resolution, thus studying

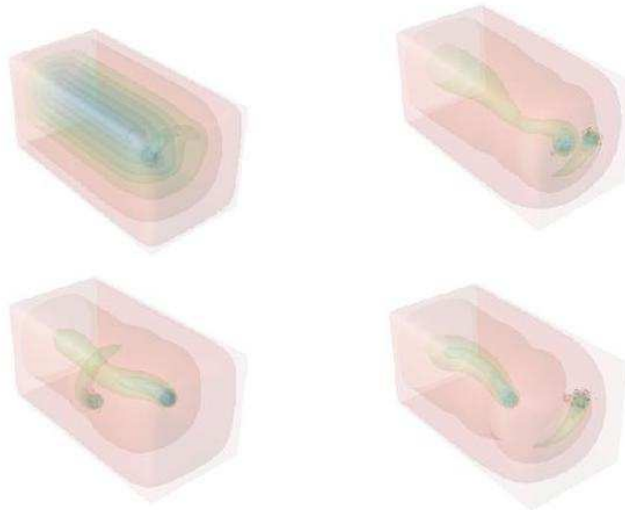


Fig. 4. Convection-Diffusion around moving balls.

the full discrete scheme. On a practical level we are working on adapting the method to take into account free motion of the bodies in order to be able to simulate fluid-particle flows.

References

- Y. Achdou and J.-L. Guermond. Convergence analysis of a finite element Projection/Lagrange-Galerkin method for the incompressible Navier-Stokes equations. *SIAM J. Numer. Anal.*, 37(3):799–826, 2000.
- S. Bertoluzza, M. Ismail, and B. Maury. Analysis of the discrete fat boundary method. in preparation.
- M. Ismail. *Simulation Numérique d'écoulements fluide-particules par la méthode de la frontière élargie*. PhD thesis (in preparation), to appear in french, Université Pierre et Marie Curie, Paris, France, 2003.
- B. Maury. A Fat Boundary Method for the Poisson problem in a domain with holes. *J. of Sci. Comput.*, 16(3):319–339, 2001.
- J. A. Nitsche and A. H. Schatz. Interior estimates for Ritz-Galerkin methods. *Math. Comp.*, 28:937–958, 1974.
- O. Pironneau. On the transport-diffusion algorithm and its applications to the Navier-Stokes equations. *Numer. Math.*, 38:309–332, 1982.

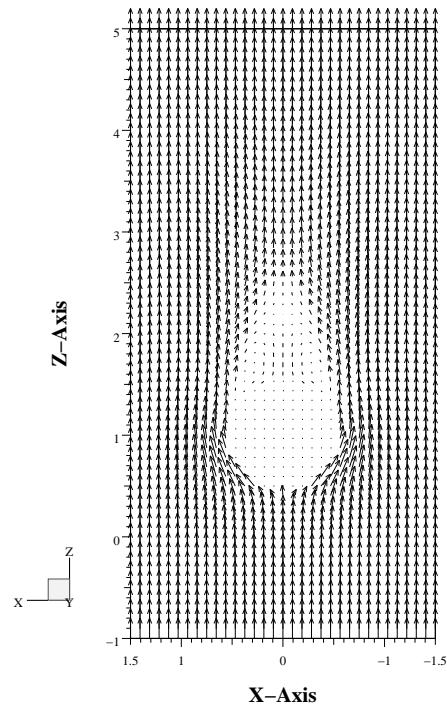


Fig. 5. Flow past a sphere at $Re = 100$.

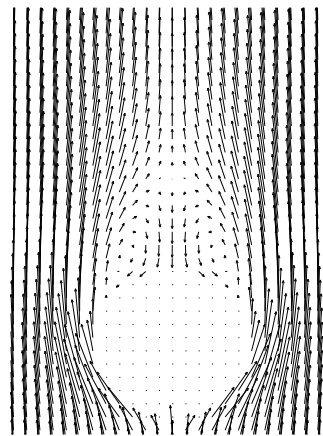


Fig. 6. Zoom.